J Mater Sci (2011) 46:4715–4718
DOI 10.1007/s10853-011-5455-2

LETTER

Tunable high Q perovskite dielectrics in the BaO–NiO–Ta_2O_5 system

Meganathan Thirumal · Peter K. Davies

Received: 11 January 2011 / Accepted: 9 March 2011 / Published online: 22 March 2011

Introduction

Oxide perovskites with the general formula $A(B^{I}_{1/3}B^{II}_{2/3})O_3$ (A = Ba, Sr; B^{I} = Mg, Zn, Ni, Co, etc.; B^{II} = Ta, Nb) have been investigated for over two decades for applications as dielectric resonators in wireless communication systems. The key materials requirements include a high dielectric constant (ε), low dielectric loss or high quality factor (Q) in the GHz range, and a zero temperature coefficient of resonant frequency (τ_f). Recent investigations of the effect of Zn volatilization on the properties of one of the most studied high Q systems, $Ba(Zn_{1/3}Ta_{2/3})O_3$ (BZT), revealed a resultant Zn-deficient impurity phase, $Ba_8ZnTa_6O_{24}$ also exhibits a good microwave response ($\varepsilon = 30.5$, $Q{\cdot}f = 62{,}000$, $\tau_f = +36$ ppm/°C) [1–3]. This phase, which has a closely related hexagonal perovskite structure (Fig. 1), can also be sintered at temperatures significantly lower than its cubic perovskite counterpart.

While the positive value of τ_f precludes the use of $Ba_8ZnTa_6O_{24}$ for commercial resonator applications, it is possible additives could tune τ_f to a zero value. Isotypic hexagonal perovskites containing other transition metal cations instead of Zn (e.g., Ni, Co) can be stabilized and have high Q values, however, they also have positive values of τ_f [4, 5]. Although the positive τ_f of $Ba_8NiTa_6O_{24}$ and $Ba_8CoTa_6O_{24}$ precludes direct tuning of the hexagonal systems, their cubic perovskite counterparts ($Ba(Ni_{1/3}Ta_{2/3})O_3$ and $Ba(Co_{1/3}Ta_{2/3})O_3$) have negative τ_f's. This offers an opportunity for tuning their temperature coefficient via the formation of two-phase hexagonal/cubic perovskite "composites". With that goal in mind, this study describes an investigation of the phase compatibility and dielectric properties of the nickel-based $(1-x)Ba(Ni_{1/3}Ta_{2/3})O_3$–$(x)$ "$Ba(Ni_{1/8}Ta_{3/4})O_3$" (=$Ba_8NiTa_6O_{24}$) system.

Experimental

Samples of $Ba_8NiTa_6O_{24}$, $Ba_8CoTa_6O_{24}$, and compositions within the $(1-x)Ba(Ni_{1/3}Ta_{2/3})O_3$–$(x)Ba(Ni_{1/8}Ta_{3/4})O_3$ system were prepared by standard solid state techniques from dried powders of $BaCO_3$ (99.9%, Cerac, Inc., Milwaukee, WI), NiO (99.99%, Aldrich, Milwaukee, WI), Co_3O_4 (>99%, J. T. Baker, Phillipsburg, N.J), and Ta_2O_5 (99.99%, Cerac). After weighing and mixing, the samples were ball-milled with ethanol. The dried powders were calcined at 1000 °C for about 13 h to remove CO_2 and subsequently ball-milled with ethanol. The final reactions were completed on uniaxially pressed pellets of the calcined powders heated to 1350–1475 °C for about 24–40 h, depending on the composition. The pellets were crushed, ground and isostatically pressed at 565 MPa and sintered at 1400–1500 °C; all of the ceramics were >95% of their theoretical density. For some samples a two stage sintering technique was used to avoid problems associated with exaggerated grain growth of the hexagonal perovskite phase [6].

Powder X-ray diffraction patterns were collected (Model DMAX-B diffractometer, Rigaku Co., Tokyo, Japan), using Cu Kα radiation generated at 45 kV and 30 mA. Polished and thermally etched sintered pellets were

M. Thirumal · P. K. Davies (✉)
Department of Materials Science and Engineering, University of Pennsylvania, Philadelphia, PA 19104-6272, USA
e-mail: davies@seas.upenn.edu

Present Address:
M. Thirumal
Department of Chemistry, University of Delhi, Delhi, India

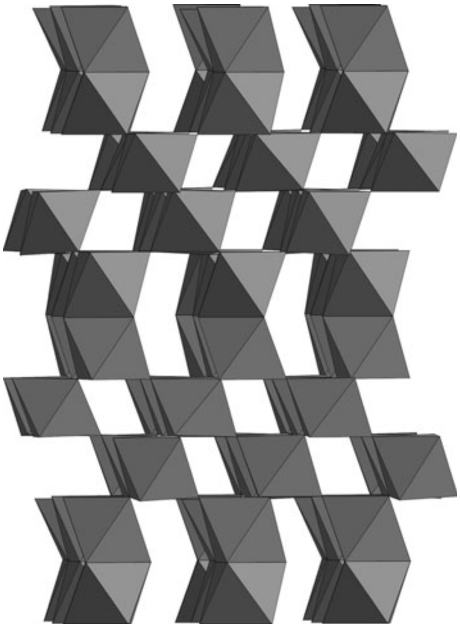

Fig. 1 8-layer hexagonal structure of $Ba_8CoTa_6O_{24}$ and $Ba_8NiTa_6O_{24}$ projected along [1$\bar{1}$0] to highlight the corner and face shared octahedra, Ba atoms are omitted for clarity

examined using a scanning electron microscope (Model 6300FV cold field-emission, JEOL, Tokyo, Japan).

The relative permittivity and dielectric loss tangent were measured in the 100 Hz to 1 MHz frequency range from −100 to 100 °C using the parallel plate method (Model HP 4284A precision LCR meter, Hewlett-Packard, Palo Alto, CA). The microwave dielectric properties were measured using the cavity method with a network analyzer (Agilent 8720ES, S-Parameter network analyzer). The $TE_{01\delta}$ mode was identified and the permittivity and unloaded Q values were calculated at resonant conditions in the reflection mode. The temperature coefficient of resonant frequency was measured by inserting the cavity inside a thermal chamber and the shift in resonant frequency was measured from 25 to 80 °C.

Results and discussion

Pure samples of $Ba_8CoTa_6O_{24}$ and $Ba_8NiTa_6O_{24}$ end members were prepared first to confirm previous reports of their positive τ_f. Single phase samples were readily obtained after heating at 1475 °C. Their X-ray patterns could be completely indexed using a cell with the same 8-layer, $(cchc)_2$, hexagonal perovskite structure reported for the Zn and Ni analogs (Fig. 1) [2, 4, 6, 7].

The dielectric properties of dense samples of $Ba_8CoTa_6O_{24}$ and $Ba_8NiTa_6O_{24}$ were measured at low frequency and in the microwave region. The dielectric constants were similar to those reported previously: $Ba_8CoTa_6O_{24}$, $\varepsilon_r = 29.7$; $Ba_8NiTa_6O_{24}$, $\varepsilon_r = 28.9$; however, the $Q{\cdot}f$ values, 39,700 at 8.8 GHz for Co and 50,900 at 8.9 GHz for Ni, were not as high as the values reported in Refs. [4, 5] (69,416 for Co and 81,758 for Ni). We also found small differences in the τ_f : $Ba_8CoTa_6O_{24}$, +33.90 ppm/°C for Co (compared to +44 in Ref. [4]) and +22.2 ppm/°C for Ni (compared to +32 in Ref. [4]). It is possible these differences are related to preferential orientation of the grains, which has been noted previously for these systems [6]. However, in agreement with the previous work τ_f for both compounds is opposite in sign to their corresponding cubic perovskites ($Ba(Co_{1/3}Ta_{2/3})O_3$, $\tau_f = -16$ ppm/°C; $Ba(Ni_{1/3}Ta_{2/3})O_3$, $\tau_f = -18$ ppm/°C) suggesting a zero τ_f microwave ceramic could exist in two-phase composites of either system [8, 9].

To confirm this hypothesis we explored the synthesis and properties of the Ni-based system: $(1-x)Ba(Ni_{1/3}Ta_{2/3})O_3$–$(x)Ba(Ni_{1/8}Ta_{3/4})O_3$. X-ray patterns collected from samples with $x = 0.0$, 0.05, 0.1, 0.2, 0.4, 0.5, 0.6, 0.8, 0.9, and 1.0 are shown in Fig. 2. The patterns for $x = 0$ ($Ba(Ni_{1/3}Ta_{2/3})O_3$) and $x = 1.0$ ($Ba_8NiTa_6O_{24}$) were in agreement with those previously reported in the literature. No evidence was found for any significant solubility for either end-member and the X-ray patterns of the intermediate compositions could all be indexed in terms of a two-phase mixture of these phases. The stable two-phase

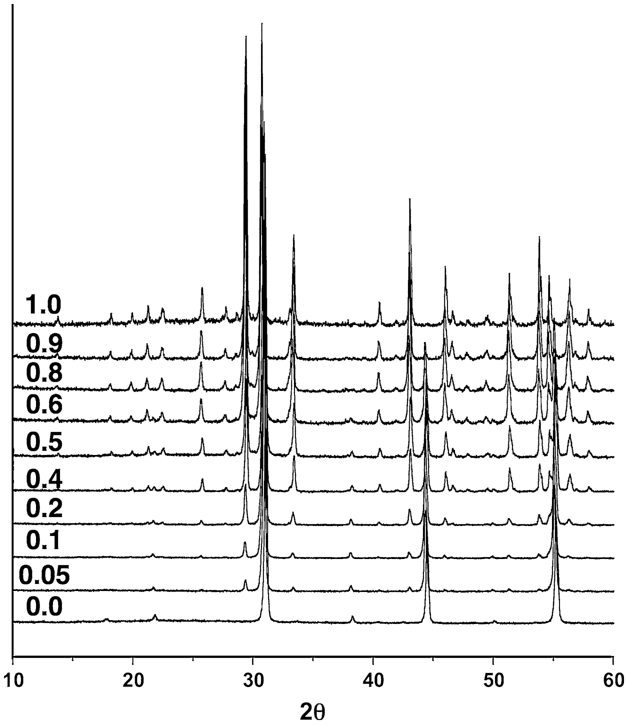

Fig. 2 Powder X-ray diffraction patterns of $(1-x)Ba(Ni_{1/3}Ta_{2/3})O_3$–$(x)Ba(Ni_{1/8}Ta_{3/4})O_3$ for $x = 0$, 0.05, 0.1, 0.2, 0.4, 0.5, 0.6, 0.8, 0.9, 1.0

existence of the cubic and hexagonal perovskite phases formed the basis for the preparation of a family of thermodynamically compatible composite structures with a tuned dielectric response.

The lower sintering temperature of $Ba_8NiTa_6O_{24}$ (1400 °C) as compared to $Ba(Ni_{1/3}Ta_{2/3})O_3$ (~1610 °C) enhanced the densification of the two-phase $(1-x)Ba(Ni_{1/3}Ta_{2/3})O_3$–$(x)Ba(Ni_{1/8}Ta_{3/4})O_3$ samples which could be sintered to >95% theoretical density at 1500 °C [9]. An SEM micrograph of the polished and thermally etched surface of a pellet with $x = 0.4$ (Fig. 3) reveals the microstructure exhibits minimal porosity and is comprised of larger grains of $Ba_8NiTa_6O_{24}$ (4–8 μm) and smaller grained $Ba(Ni_{1/3}Ta_{2/3})O_3$ (1–2 μm). The dielectric properties of the as-sintered $(1-x)Ba(Ni_{1/3}Ta_{2/3})O_3$–$(x)Ba(Ni_{1/8}Ta_{3/4})O_3$ $(0 \le x \le 1)$ ceramics are listed in Table 1. The two-phase composites show an essentially linear variation of the dielectric constant across the system. The $Q{\cdot}f$ increases with x, though the variation is not monotonic; the highest value (62,000) was recorded for $x = 0.8$.

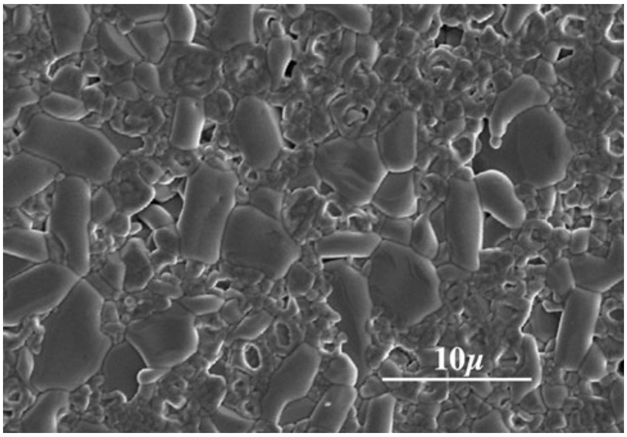

Fig. 3 SEM micrograph of $0.6Ba(Ni_{1/3}Ta_{2/3})O_3$–$0.4Ba(Ni_{1/8}Ta_{3/4})O_3$ after sintering at 1500 °C

Table 1 Microwave dielectric properties of $(1-x)Ba(Ni_{1/3}Ta_{2/3})O_3$–$(x)Ba(Ni_{1/8}Ta_{3/4})O_3$ composites

x	After sintering		After annealing (1400 °C for 48 h)		
	ε	$Q{\cdot}f$	ε	$Q{\cdot}f$	τ_f (ppm/°C)
0.05	23.2	41500 (9.7 GHz)	23.02	66349 (9.6 GHz)	−20.8
0.1	24.0	43340 (9.4 GHz)	23.68	50414 (9.8 GHz)	−10.7
0.2	23.7	38680 (9.7 GHz)	22.16	32623 (10.1 GHz)	−10.3
0.4	24.6	47750 (9.3 GHz)	24.99	61890 (9.3 GHz)	−0.4
0.5	25.1	47470 (9.4 GHz)	25.65	66682 (9.4 GHz)	+3.2
0.6	26.4	41130 (8.9 GHz)	26.25	54189 (9.03 GHz)	+7.8
0.8	28.2	61750 (8.9 GHz)	27.82	65286 (9.03 GHz)	+22.3
0.9	28.0	54220 (8.7 GHz)	27.65	68683 (8.9 GHz)	+23.0
1.0	28.9	50870 (9.0 GHz)	28.59	63000 (9.0 GHz)[a]	+22.2

[a] Annealed at 1325 for 48 h

The dielectric loss of the $A(B^{I}_{1/3}B^{II}_{2/3})O_3$ family of microwave perovskites is well known to respond to slow cooling or post-sintering lower temperature annealing [10]. These changes are associated with alterations in the ordering of the cations on the B-site sub-lattice through enhanced positional order and/or increases in the size of the different orientational domains of their 1:2 ordered structure [10–12]. Therefore, the sintered pellets were annealed for 48 h at 1400 °C and their structure and dielectric properties were re-examined. While the lower temperature treatment had no significant effect on the dielectric constant the $Q{\cdot}f$ values increased significantly, particularly for the $Ba(Ni_{1/3}Ta_{2/3})O_3$-rich compositions, see Table 1. To ascertain the effect of the annealing on the chemical ordering in the $Ba(Ni_{1/3}Ta_{2/3})O_3$ component, X-ray diffraction patterns were collected from the top and bottom surface of the pellets before and after annealing. Figure 4 shows the X-ray data collected from a sample with $x = 0.05$. The width of the superstructure peaks from the chemical ordering show a clear decrease after the heat treatment and the integrated intensity of the ordering reflections show a small increase. The increase in $Q{\cdot}f$ for these samples is therefore consistent with the previous observations of improvements in Q with enhanced chemical order.

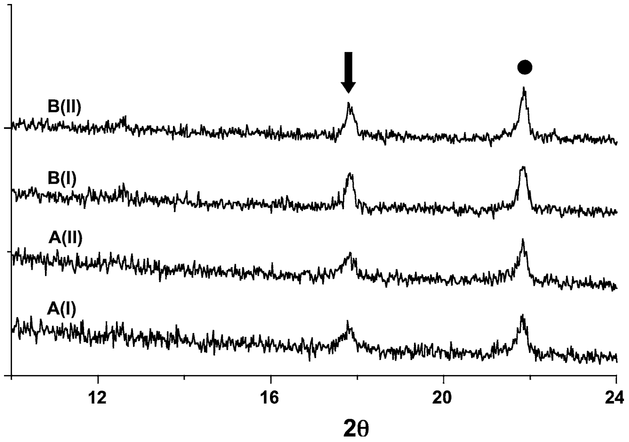

Fig. 4 Low angle region of the X-ray diffraction patterns of the top (I) and bottom (II) surfaces of (0.95) $Ba(Ni_{1/3}Ta_{2/3})O_3$–(0.05) $Ba(Ni_{1/8}Ta_{3/4})O_3$ pellets: (*A*) after sintering; (*B*) after annealing at 1400 for 48 h. *Arrow* highlight the (100) superstructure reflection, *circle* represents the fundamental reflection

After the lower temperature annealing the samples with higher x values, i.e., $Ba_8NiTa_6O_{24}$-rich composites, also show improvements in their $Q{\cdot}f$ (Table 1). Although part of the enhanced $Q{\cdot}f$ could be associated with increased cation order in the minority $Ba(Ni_{1/3}Ta_{2/3})O_3$ phase, the improvement for these samples and pure $Ba_8NiTa_6O_{24}$ indicates other factors must also be involved. We investigated the effect of annealing on the microstructure of $Ba_8NiTa_6O_{24}$ by comparing the microstructure of the as-sintered samples to those annealed for extended periods at lower temperature (in this case 1325 °C). As shown in Fig. 5 the extended annealing induces significant grain growth with the length and width of the "bar-shaped" grains increasing from $\sim 10 \times 2$ to $>100 \times 20$ μm. Consistent with previous studies, it is also evident the grains of $Ba_8NiTa_6O_{24}$ show considerable preferential orientation [6]. We believe these factors combined are responsible for the small improvements in $Q{\cdot}f$ observed after annealing composites where $Ba_8NiTa_6O_{24}$ is the majority phase.

The variation of τ_f in the two-phase composites, Table 1, is an essentially linear function of composition. As conjectured, given the opposite sign of τ_f for the two end members the temperature coefficient can be tuned to a zero value. Our experiments indicate the zero value occurs at a composition with $x = 0.4$. This zero τ_f ceramic has $\varepsilon = 24.6$ and $Q{\cdot}f = 47{,}700$.

It is likely the utility of these perovskites in permitting the design of high Q, zero τ_f cubic/hexagonal composites could be extended to other tantalate and niobate based systems. In particular the Co tantalate system, where the end members also have opposite signs of τ_f, would be a logical candidate for study.

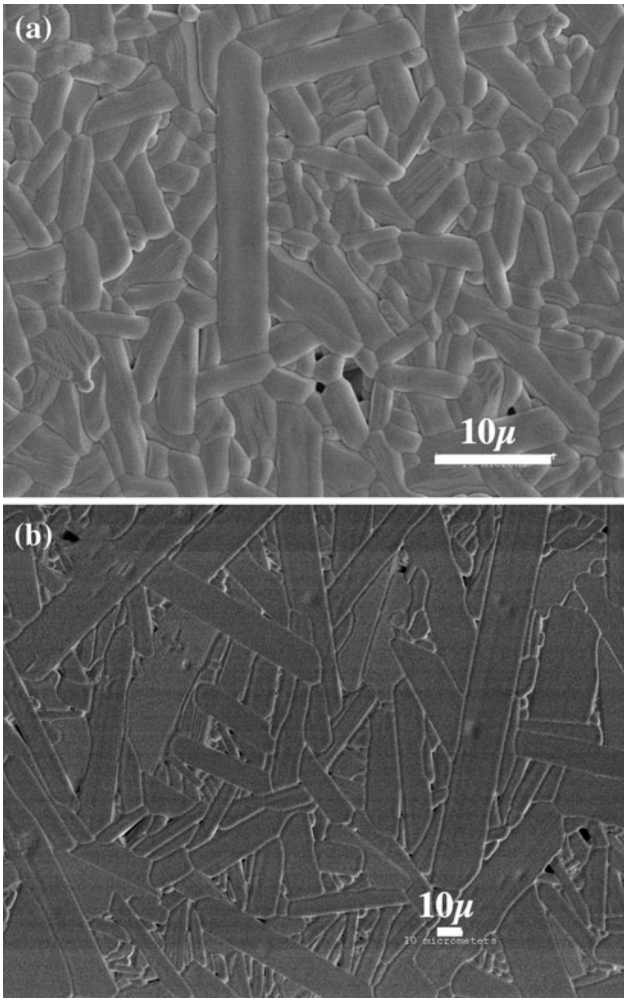

Fig. 5 SEM micrograph of $Ba_8NiTa_6O_{24}$: **a** after sintering; **b** after a subsequent anneal at 1325 °C for 48 h

Conclusions

Compositions lying between $Ba(Ni_{1/3}Ta_{2/3})O_3$ and $Ba_8NiTa_6O_{24}$ (=$Ba(Ni_{1/8}Ta_{3/4})O_3$ were prepared and investigated. X-ray diffraction revealed these samples form stable two-phase mixtures of the respective cubic and hexagonal end members. Measurement of the dielectric properties at microwave frequencies demonstrated the temperature coefficient of the resonant frequency of the two-phase composites could be tuned to a zero value. The zero τ_f ceramic has $\varepsilon = 24.6$ and a high $Q{\cdot}f = 47{,}700$. The quality factors could be improved through a post-sintering annealing treatment that enhances the ordering of the cubic perovskite component and increases the grain size of the hexagonal end-member.

Acknowledgements This work was supported by Ericsson Radio Access and made use of the MRSEC shared experimental facilities supported by the National Science Foundation through Grant No. DMR 05-20020.

References

1. Davies PK, Borisevich A, Thirumal M (2003) J Eur Ceram Soc 23:2461
2. Moussa SM, Claridge JB, Rosseinsky MJ, Clarke S, Ibberson RM, Price T, Iddles DM, Sinclair DC (2003) Appl Phys Lett 82:4537
3. Bieringer M, Moussa SM, Liam DL, Burrows A, Kiely CJ, Rosseinsky MJ, Ibberson RM (2003) Chem Mater 15:586
4. Kan A, Ogawa H, Yokoi A, Ohsato H (2006) Jpn J Appl Phys 45:7494
5. Kawaguchi S, Ogawa H, Kan A, Ishihara S (2006) J Eur Ceram Soc 26:2045
6. Thirumal M, Davies PK (2005) J Am Ceram Soc 88:2126
7. Abakumov AM, Van Tendeloo G, Scheglov AA, Shpanchenko RV, Antipov EV (1996) J Solid State Chem 125:102
8. Tamura H, Konoike T, Sakabe Y, Wakino K (1984) J Am Ceram Soc 67:C-59
9. Kolodiazhnyi T, Petric A, Belous A, V'Yunov O, Yanchevskij O (2002) J Mater Res 17:3182
10. Davies PK, Tong J, Negas T (1997) J Am Ceram Soc 80:1727
11. Wu H, Davies PK (2006) J Am Ceram Soc 89:2239
12. Wu H, Davies PK (2006) J Am Ceram Soc 89:2250